

Supporting Material

Biomimetic zinc chlorin – poly(4-vinylpyridine) assemblies: doping level dependent emission-absorption regimes

Ville Pale,^{a,‡} Taru Nikkonen,^{b,‡} Jaana Vapaavuori,^c Mauri Kostiainen,^c Jari Kavakka,^b Jorma Selin,^a Ilkka Tittonen^{a,*} and Juho Helaja^{b,*}

^a Department of Micro and Nanosciences, Aalto University, P.O. Box 13500, FI-00076 Aalto, Finland

^b Laboratory of Organic Chemistry, Department of Chemistry, P.O. Box 55, FI-00014 University of Helsinki, Finland

^c Department of Applied Physics, Aalto University, P.O. Box 15100, FI-00076 Aalto, Finland

* Corresponding authors.

‡ These authors contributed equally to this work.

| | | |
|---|---|---|
| 1 | Diffusion ordered spectroscopy (DOSY) of ZnPPME – P4VP assemblies | 2 |
| 2 | Small angle X-ray scattering (SAXS) and transmission electron microscopy (TEM) data of PS- <i>b</i> -P4VP(ZnPPME) _{1.0} | 3 |
| 3 | Semiempirical molecular modeling of a P4VP fragment | 4 |
| 4 | Scanning electron microscope (SEM) data of spin-coated Zn PPME – P4VP thin films on a glass substrate | 5 |
| 5 | Fluorescence lifetime decays for P4VP(ZnPPME) and P4VP(Zn-3 ¹ -OH-PPME) assemblies | 5 |
| 6 | Intermolecular chlorin-chlorin distances (<i>R</i>) in chlorin - P4VP assemblies and Förster distance (<i>R</i> ₀) | 6 |

1 Diffusion ordered spectroscopy (DOSY) of ZnPPME – P4VP assemblies

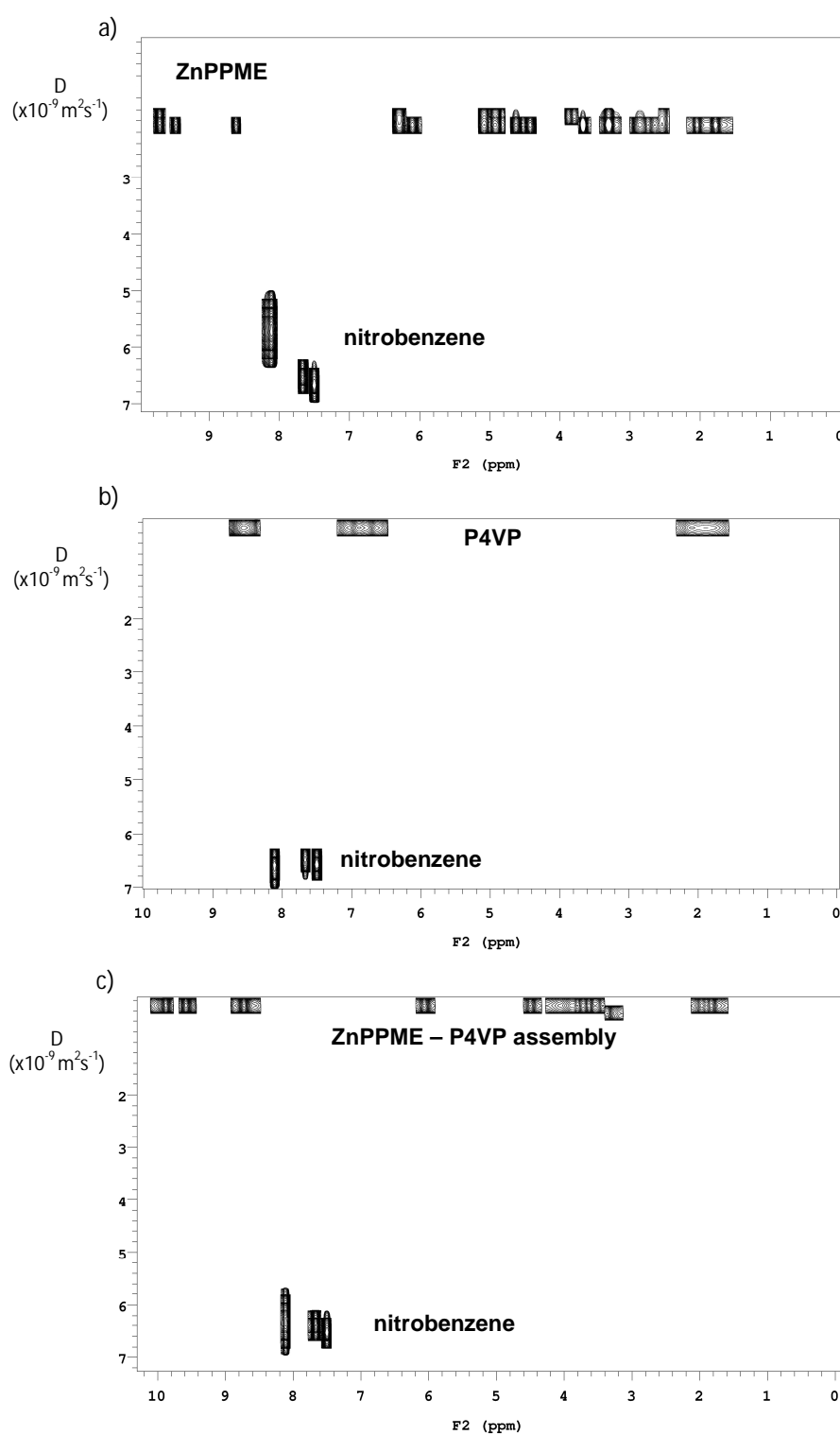


Fig. S1 DOSY spectra of (a) Zn *pyro*-pheophorbide *a* methylester (10 mM) (b) P4VP (polymer 52.6 μM ; the molarity of pyridine units in polymer backbone is 30 mM) (c) 1:3 mixture of Zn *pyro*-pheophorbide *a* methylester (10 mM) and P4VP (polymer 52.6 μM ; the molarity of pyridine units in polymer backbone is 30 mM) measured in d_5 -nitrobenzene.

2 Small angle X-ray scattering (SAXS) and transmission electron microscopy (TEM) data of PS-*b*-P4VP(ZnPPME)_{1.0}

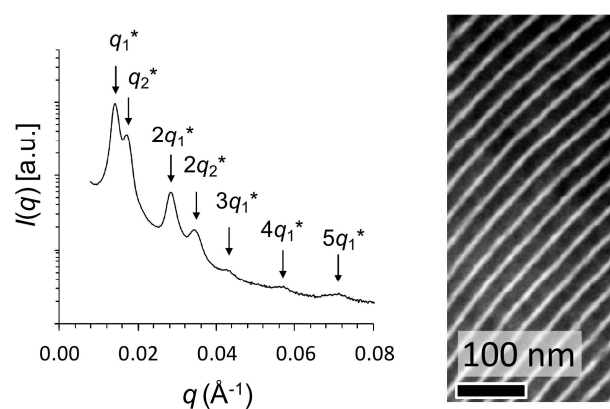


Fig. S2 Small angle X-ray scattering and transmission electron microscopy data of PS-*b*-P4VP(ZnPPME)_{1.0} showing a lamellar morphology. SAXS indicates lamellar morphology with two different long periods (44.2 nm and 36.8 nm). Due to the high molecular weight ratio between the ZnPPME and pyridine repeating units, macrophase separation is likely at high complexation ratios.

3 Semiempirical molecular modeling of a P4VP fragment

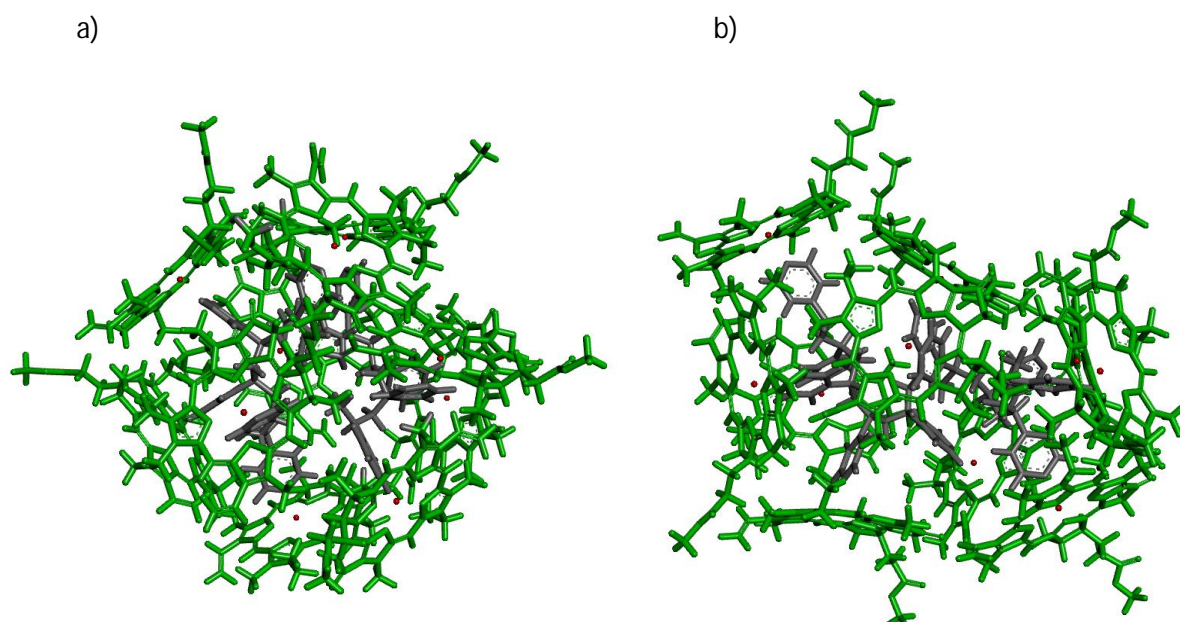


Fig. S3 Two PM6 geometry optimized Zn chlorin – P4VP systems a) and b) consisting of 10*pyridyl and 10* ZnPPME units illustrates that a number of different assemblies at 1:1 host-guest loading level are possible without limiting geometrical restrictions i.e. each Zn atom in chlorin rings are coordinated by pyridine electron pairs. Both optimizations were started from arbitrary geometry except that pyridine units were set into proximity of Zn atoms ($< 2.5 \text{ \AA}$). In both cases each pyridine unit (gray colored) is coordinated to Zn (red) of chlorin (green).

The computations were run with Gaussian 09 software (Revision09 C.01) without solvation model.¹

¹ Gaussian 09, Revision A.01; M. J. Frisch, G. W. Trucks, H. B. Schlegel, G. E. Scuseria, M. A. Robb, J. R. Cheeseman, G. Scalmani, V. Barone, B. Mennucci, G. A. Petersson, H. Nakatsuji, M. Caricato, X. Li, H. P. Hratchian, A. F. Izmaylov, J. Bloino, G. Zheng, J. L. Sonnenberg, M. Hada, M. Ehara, K. Toyota, R. Fukuda, J. Hasegawa, M. Ishida, T. Nakajima, Y. Honda, O. Kitao, H. Nakai, T. Vreven, J. A. Montgomery, Jr., J. E. Peralta, F. Ogliaro, M. Bearpark, J. J. Heyd, E. Brothers, K. N. Kudin, V. N. Staroverov, R. Kobayashi, J. Normand, K. Raghavachari, A. Rendell, J. C. Burant, S. S. Iyengar, J. Tomasi, M. Cossi, N. Rega, J. M. Millam, M. Klene, J. E. Knox, J. B. Cross, V. Bakken, C. Adamo, J. Jaramillo, R. Gomperts, R. E. Stratmann, O. Yazyev, A. J. Austin, R. Cammi, C. Pomelli, J. W. Ochterski, R. L. Martin, K. Morokuma, V. G. Zakrzewski, G. A. Voth, P. Salvador, J. J. Dannenberg, S. Dapprich, A. D. Daniels, O. Farkas, J. B. Foresman, J. V. Ortiz, J. Cioslowski, D. J. Fox, Gaussian, Inc., Wallingford CT, 2009.

4 Scanning electron microscope (SEM) data of spin-coated Zn PPME – P4VP thin films on a glass substrate

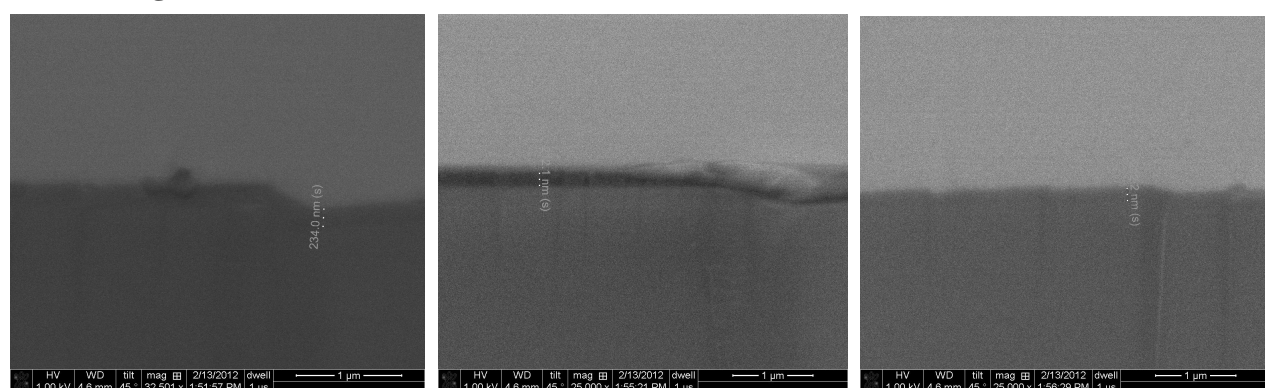


Fig. S4 Cross sectional SEM images from the Zn chlorin – P4VP thin film. The left picture shows the cross section from the center of the sample, whereas the pictures in the right are from the sides.

5 Fluorescence lifetime decays for P4VP(ZnPPME) and P4VP(Zn- $^{31}\text{-OH}$ -PPME) assemblies

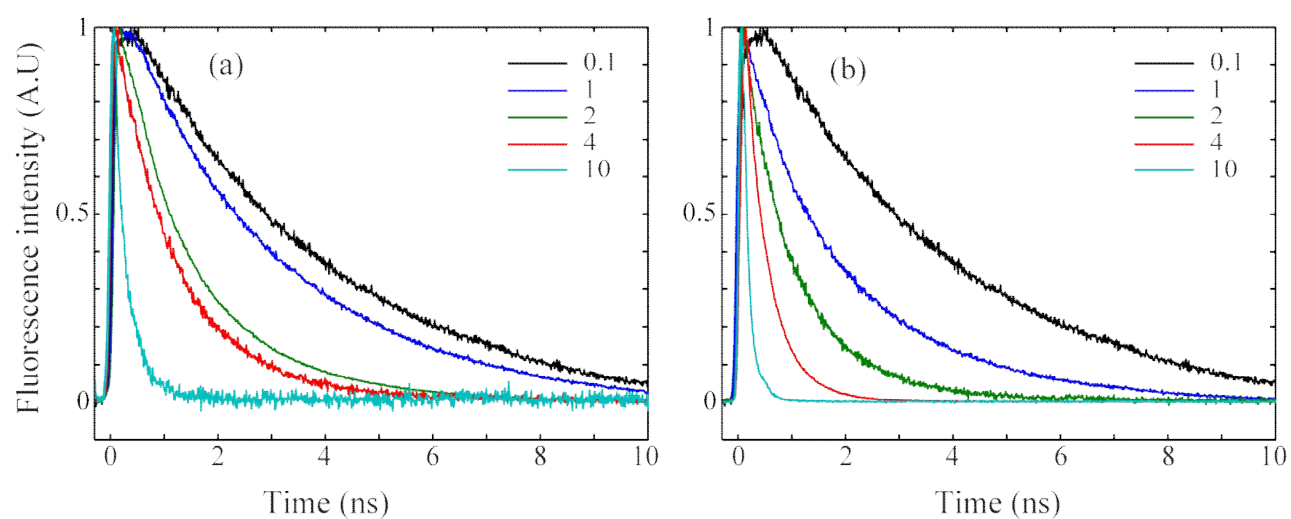


Fig. S5 The measured fluorescence lifetime decays normalized to unity for (a) P4VP(ZnPPME) and (b) P4VP(Zn- $^{31}\text{-OH}$ -PPME) assemblies with different doping levels (wt%).

6 Intermolecular chlorin-chlorin distances (R) in chlorin - P4VP assemblies and Förster distance (R_0)

In the microscopic approximation, the dye loading values were transformed to intermolecular distances using a following spherical unit cell approximation $R = 2(3V/4\pi)^{1/3}$, where $V = V_{dye}N_{dye} + V_{P4VP}N_{P4VP}$ with following Connolly solvent excluded volumes: $V_{P4VP} = 100 \text{ \AA}^3$, $V_{Zn-3^1-OH-PPME} = 507.488 \text{ \AA}^3$ and $V_{ZnPPME} = 489.241 \text{ \AA}^3$. These volumes were obtained using Chem3D and with probe radius of 1.4 Å.

Table. S1 Transformation of dye loading values to intermolecular distances using microscopic approximation.

| wt% | chlorin – pyridine ratio in dye-polymer assembly | | $V = V_{dye}N_{dye} + V_{P4VP}N_{P4VP} (\text{\AA}^3)$ | | Intermolecular distance, R (Å) | |
|------|--|-------------------------------|--|----------------------------------|----------------------------------|----------------------------------|
| | N_{ZnPPME}/N_{P4VP} | $N_{Zn-3^1-OH-PPME}/N_{P4VP}$ | dye = ZnPPME | dye = Zn-3 ¹ -OH-PPME | dye = ZnPPME | dye = Zn-3 ¹ -OH-PPME |
| 0.1 | 1 : 5815 | 1 : 5987 | 581989.241 | 599207.488 | 103.5870 | 104.5987 |
| 0.25 | 1 : 2323 | 1 : 2391 | 232789.241 | 239607.488 | 76.3229 | 77.0609 |
| 0.5 | 1 : 1158 | 1 : 1193 | 116289.241 | 119807.488 | 60.5592 | 61.1639 |
| 1 | 1 : 576 | 1 : 593 | 58089.241 | 59807.488 | 48.0506 | 48.5198 |
| 2 | 1 : 285 | 1 : 294 | 28989.241 | 29907.488 | 38.1136 | 38.5118 |
| 4 | 1 : 140 | 1 : 144 | 14489.241 | 14907.488 | 30.2470 | 30.5353 |
| 6 | 1 : 91 | 1 : 94 | 9589.241 | 9907.488 | 26.3590 | 26.6474 |
| 8 | 1 : 67 | 1 : 69 | 7189.241 | 7407.488 | 23.9457 | 24.1856 |
| 10 | 1 : 52 | 1 : 54 | 5689.241 | 5907.488 | 22.1489 | 22.4286 |

In the macroscopic approximation, the chromophore number density² was first calculated with a formula $\# = \frac{w_i \rho N_A}{M_i}$, where w_i is the weight fraction of the chromophore i (wt%), ρ is the density of the material (1.20 g/cm³), N_A is the Avogadro constant and M_i is the molar mass of dye i . The inverse of this value ($\#^{-1}$) denotes the average space reserved by one dye molecule. Therefore, the cubic root of $\#^{-1}$ gives the distance between the chromophores in a cubic lattice.

Table. S2 Transformation of dye loading values to intermolecular distances using macroscopic approximation.

| wt% | Chromophore number density, $\#$ (1/cm ³) | | Intermolecular distance, R (Å) | |
|------|--|----------------------------------|----------------------------------|----------------------------------|
| | dye = ZnPPME | dye = Zn-3 ¹ -OH-PPME | dye = ZnPPME | dye = Zn-3 ¹ -OH-PPME |
| 0.1 | 1.102E+18 | 1.07044E+18 | 96.8143 | 97.7567 |
| 0.25 | 2.755E+18 | 2.67609E+18 | 71.3334 | 72.0277 |
| 0.5 | 5.51E+18 | 5.35218E+18 | 56.6173 | 57.1684 |
| 1 | 1.102E+19 | 1.07044E+19 | 44.9372 | 45.3746 |
| 2 | 2.204E+19 | 2.14087E+19 | 35.6667 | 36.0139 |
| 4 | 4.408E+19 | 4.28175E+19 | 28.3087 | 28.5842 |
| 6 | 6.612E+19 | 6.42262E+19 | 24.7299 | 24.9706 |
| 8 | 8.816E+19 | 8.56349E+19 | 22.4686 | 22.6873 |
| 10 | 1.102E+20 | 1.07044E+20 | 20.8580 | 21.0610 |

At small doping levels the difference between these approximations is significant, which is however reduced with higher chlorin concentrations. Thus, these approximations yield roughly the same values for the intermolecular distances especially at high doping values.

² P. A. Sullivan, H. Rommel, Y. Liao, B. C. Olbricht, A. J. P. Akelaitis, K. A. Firestone, J-W. Kang, J. Luo, J. A. Davies, D. H. Choi, B. E. Eichinger, P. J. Reid, A. Chen, A. K-Y. Jen, B. H. Robinson and L. R. Dalton, *J. Am. Chem. Soc.*, 2007, **129**, 7523-7530

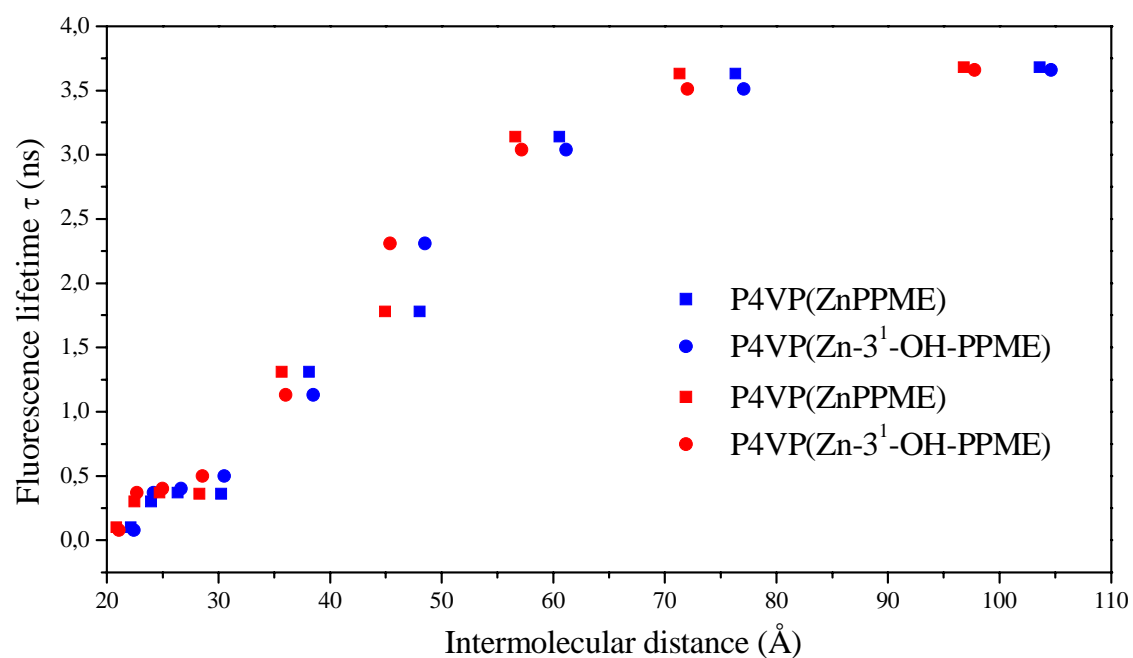


Fig. S6 The fluorescence lifetimes for P4VP(ZnPPME) and P4VP(Zn-3¹-OH-PPME) assemblies given as the function of the intermolecular distance. Intermolecular distances were obtained by using microscopic (blue) and macroscopic (red) approximations.

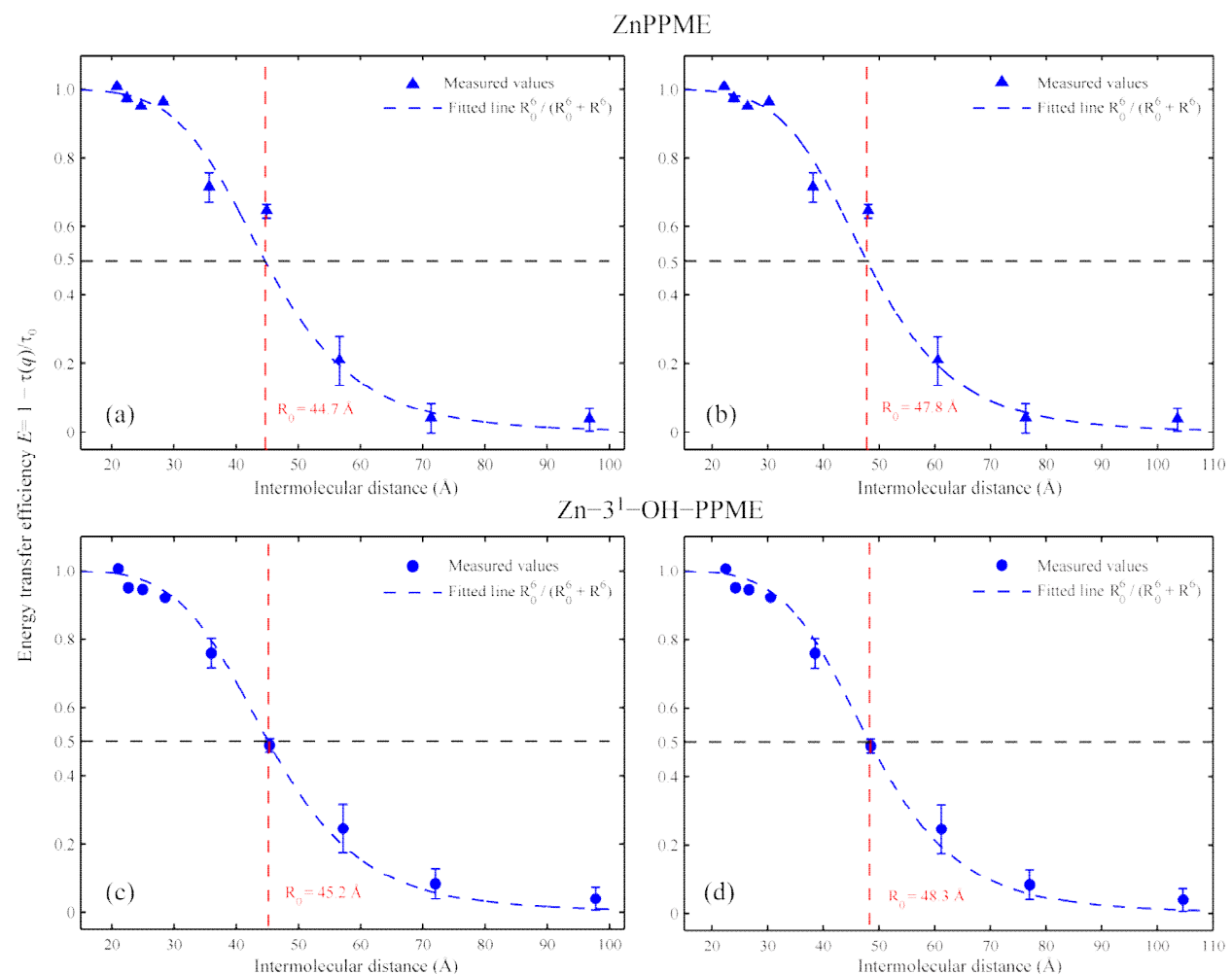


Fig. S7 The energy transfer efficiency as the function of the intermolecular distance for ZnPPME (a-b) and Zn-3¹-OH-PPME (c-d) dyes in P4VP using both macroscopic (a and c) and microscopic (b and d) approximations. The Förster distance (R_0) was determined for both dyes by fitting the energy transfer function $f(R)=R_0^6 / R_0^6+R^6$ to the measured data.

The efficiency of the energy transfer³ was determined using the fluorescence lifetimes with following equation

$$E = 1 - \frac{\tau(q)}{\tau_0},$$

where τ_0 is the lifetime measured at 0.1 wt% doping level and $\tau(q)$ are the different fluorescence lifetime values as the function of the doping level. The point where the efficiency has decayed to half of its original value should denote the Förster distance. Using this, we defined from the measured data the Förster distances for both dyes using macroscopic approximation, which yielded values 44.7 Å and 45.2 Å for ZnPPME and Zn-3¹-OH-PPME, respectively. Microscopic approximation resulted Förster distances 47.8 Å and 48.3 Å for ZnPPME and Zn-3¹-OH-PPME, respectively.

³ J. R. Lakowicz, in *Principles of fluorescence spectroscopy*, Kluwer Academic/Plenum Publishers, New York, 2nd edn., 1999, ch. 13. pp. 443-475.